

The Causes of Horizontal-Vertical (H-V) Bias in Optical Lithography: Dipole Source Errors

John J. Biafore, Chris A. Mack*, Stewart A. Robertson, Mark D. Smith, Sanjay Kapasi
KLA-Tencor, FINLE Division
*www.lithoguru.com

Abstract

Horizontal-Vertical (H-V) bias is the systematic difference in linewidth between closely located horizontally and vertically oriented resist features that, other than orientation, should be identical. There are two major causes of H-V bias: astigmatism, which causes an H-V bias that varies through focus, and illumination source errors such as telecentricity error. In this paper, the effects of simple dipole source errors upon H-V bias and placement error through focus are explored through simulation.

Keywords: H-V bias, dipole, CD control, lithography modeling, PROLITH

1. Introduction

H-V bias is the systematic difference in linewidth between closely located horizontally and vertically oriented resist features that, other than orientation, should be identical. H-V bias has always been a concern in optical lithography, but it has tended to be one of the “second order” errors that rarely limits overall lithographic capability. It’s not clear, however, whether H-V bias will retain its second tier status in the 65nm and 45nm generations, or graduate to a first tier concern.

There are two main causes of H-V bias. The most well known cause, covered in the first paper in this series, is astigmatism and related aberrations¹. The second is illumination source shape error, such as illumination telecentricity error caused by a source not centered in the pupil. Source shape errors in the context of the simple dipole are explored further in this paper.

2. Simple Dipole Source

Consider a dipole source with circular poles oriented symmetrically about the origin and positioned upon the x -axis of the pupil. The diffraction pattern of vertical, y -oriented lines will spread across the x -axis of the pupil, corresponding to $\theta = 0^\circ$ and 180° while the diffraction pattern of horizontal, x -oriented lines will spread along the across the y -axis of the pupil, corresponding to $\theta = 90^\circ$ and 270° . We may adjust the center of the pole positions in the pupil (the dipole center sigma), such that 100% 2-beam imaging may be achieved for a given mask pitch of vertically y -oriented lines by:

$$\sigma_{Center} = \frac{\lambda}{2 NA pitch} \quad (1)$$

Figure 1a shows a graphical example of the resulting diffraction pattern of a vertical line. Matching of the source diffraction pattern for the vertical lines produces interference of the left pole of the 0 order with right pole of the -1 order and interference of the right pole of the 0 order with left pole of the +1 order. The alignment of the source diffraction pattern by adjustment of center sigma using equation (1) produces 100% 2-beam imaging (0,-1 & 0,+1 orders).

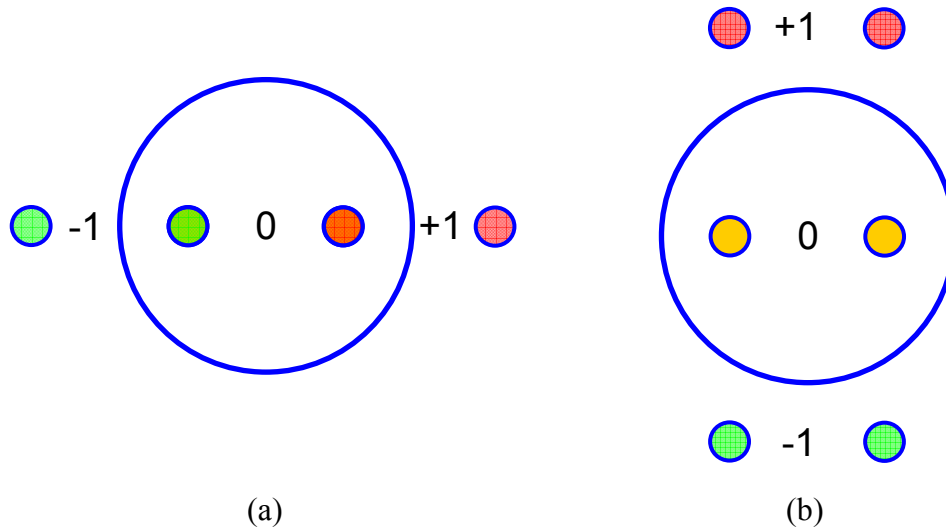


Figure 1. Example of dipole source diffraction patterns for a) vertical (y -oriented) lines with dipole center sigma adjusted to produce 100% 2-beam imaging and high contrast imaging, and b) horizontal (x -oriented) lines of the same mask pitch; only the zero order is transmitted yielding irradiance only

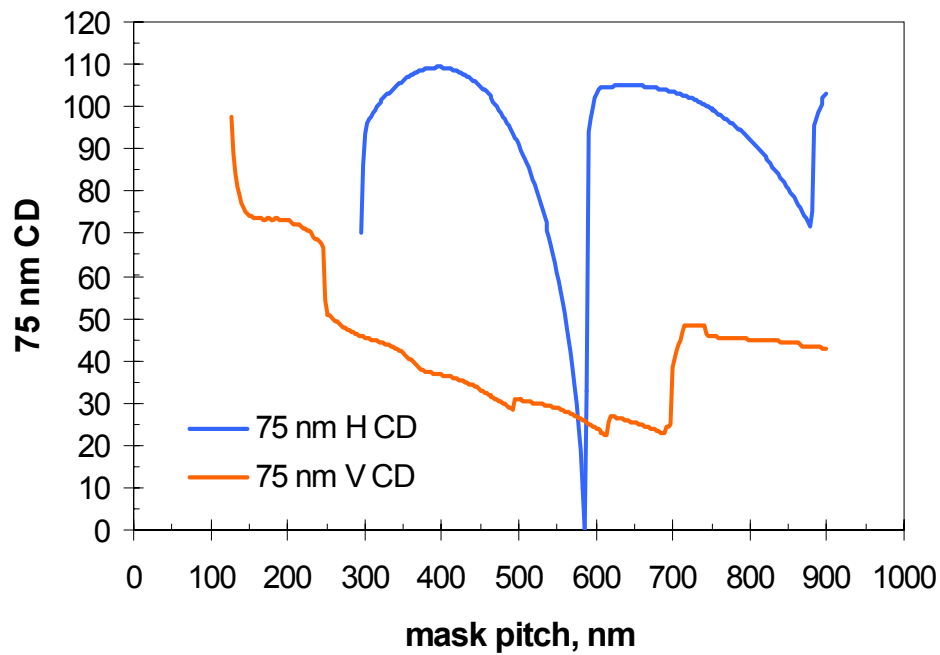
Figure 1b shows a graphical example of the resulting diffraction pattern for horizontal lines of the same mask pitch. Quite simply, vertical y -oriented lines at this pitch image quite well with the dipole configuration, while horizontal x -oriented lines won't image at all, since only the 0 order is transmitted. If the dipole source poles are points oriented symmetrically about the origin on the x -axis of the pupil, the minimum pitch that will image for a vertical y -oriented line is:

$$Vertical\ pitch_{min} = \frac{\lambda}{NA(1 + \sigma_{Center})} \quad (2)$$

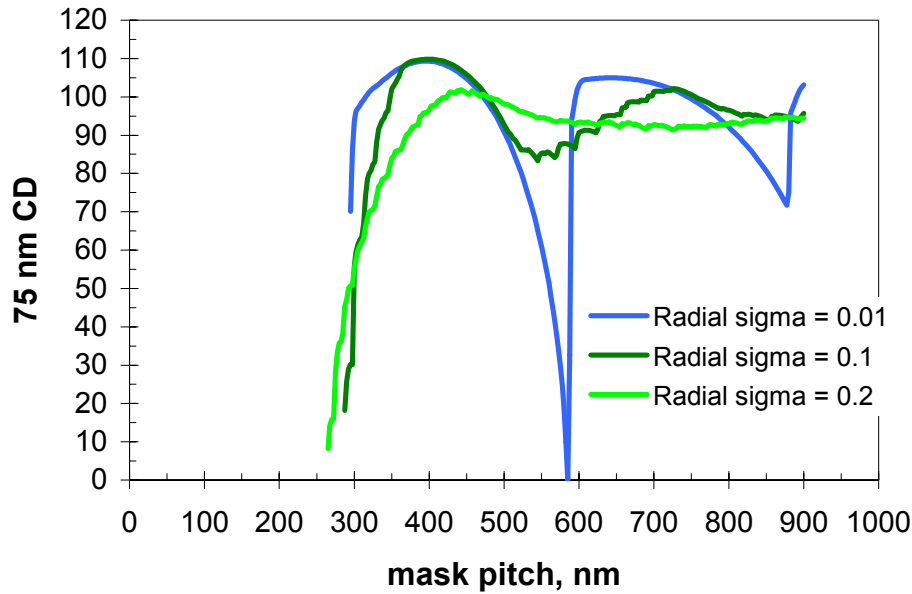
The minimum pitch that will image for a horizontal x -oriented line is:

$$Horizontal\ pitch_{min} = \frac{\lambda}{NA\sqrt{1 - \sigma_{Center}^2}}, \quad \sigma < 1 \quad (3)$$

As an example, consider the case where $\lambda = 193$ nm, NA = 0.92, dipole center $\sigma = 0.7$, radial $\sigma = 0.01$ (i.e., a point dipole). The minimum vertically-oriented pitch that will image is approximately ~ 125 nm; conversely, the minimum horizontal pitch that will image is ~ 295 nm. Figure 2a shows a plot of vertical and horizontal 75 nm line CD as a function of mask pitch with the above illuminator. Figure 2b shows CD vs. pitch with the same conditions used in Figure 2a, yet also includes the effect of dipole radial σ (pole radius). CD vs. pitch behavior is ‘smoothed’ by increasing radial σ . The impact of dipole radius or, more generally, dipole source shape, on CD vs. pitch behavior is clearly important, but not considered further in this work.



(a)



(b)

Figure 2 (a) Example of simulated horizontal (x -oriented) and vertical (y -oriented) 75 nm line vs. mask pitch using $\lambda = 193$ nm, 0.92 NA, nominal dipole center $\sigma = 0.7$, radial $\sigma = 0.1$. The minimum resolved horizontal (x -oriented) pitch in this case is about 295 nm while the minimum resolved vertical (y -oriented) pitch is about 125 nm. (b) Effect of dipole radial sigma upon horizontal 75 nm lines vs. pitch using the same illumination conditions. CD vs. pitch behavior is smoothed and minimum resolved pitch is decreased.

3. Simulation Procedure for the Study

The effect of dipole source errors upon Horizontal CD, Vertical CD, H-V bias, and placement error through focus are explored through resist simulation with PROLITH v9.3.3. A 75 nm CD, 150 nm pitch anchoring process is simulated with illumination conditions producing 100% 2-beam imaging ($k_1=0.37$). This process generally represents the high contrast imaging present in a memory cell. The horizontal and vertical CDs, H-V bias and placement errors through focus produced by dipole source errors are monitored for a larger line CD and range of pitch; in this case, 100 nm H & V CDs with pitch range 300 nm – 500 nm are chosen ($k_1 = 0.48$, $k_{pitch} = 1.4 - 2.4$). The 100 nm features generally represent H & V features on the periphery of the memory cell.

The dipole source errors considered here are:

- x -telecentricity error, dipole shifted horizontally relative to pupil
- y -telecentricity error, dipole shifted vertically relative to pupil
- unbalanced pole intensity, left pole intensity is 50%, right pole intensity is 100%
- rotational error, dipole rotated by 5 degrees

4. Inherent H-V bias with Dipole and Mask OPC

Figure 3 shows the large process window obtained for the 75 nm CD, 150 nm pitch anchoring process when no source errors are applied. The process window shows 0.8 μm DOF at 10% exposure latitude. However, a very large H-V bias is observed for the uncorrected 100 nm features. Generally, 100 nm vertical (y -oriented) features undersize 20% - 40% of target while 100 nm horizontal (x -oriented) oversize 15% - 65% of target. Figure 4 shows the resist CDs vs. pitch for H & V 100 nm mask features.

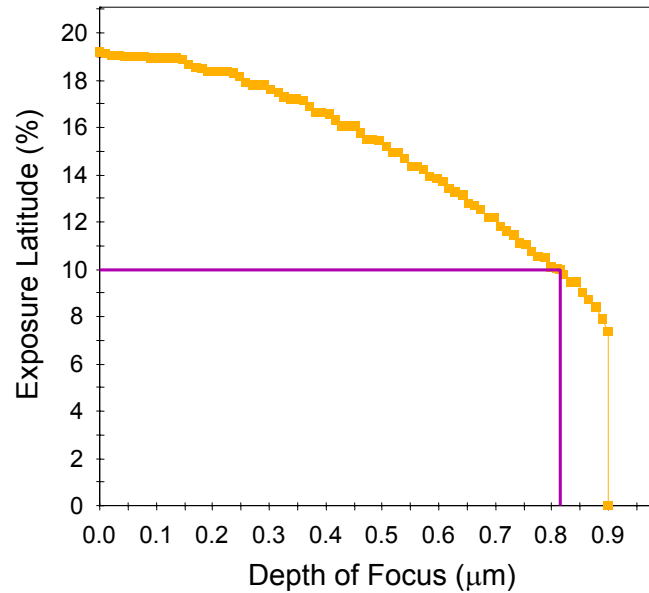


Figure 3. Process window results for the anchor process: vertical (y -oriented) 75 nm lines, 150 nm pitch ($\lambda = 193$ nm, 0.92 NA, nominal dipole center $\sigma = 0.7$, radial $\sigma = 0.1$).

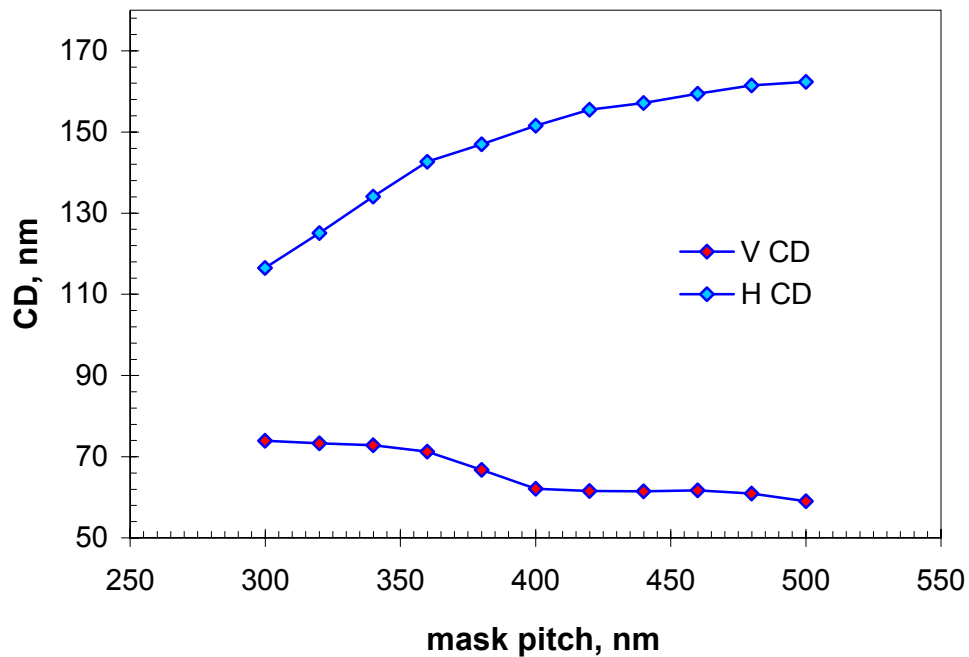


Figure 4. Horizontal and vertical CDs for a nominal 100 nm feature size through pitch, produced by dipole. No mask bias or source errors are applied ($\lambda = 193$ nm, 0.92 NA, nominal dipole center $\sigma = 0.7$, radial $\sigma = 0.1$).

The mask bias needed to achieve 100 nm in both H & V from 300 nm – 500 nm pitch is about -27.5 nm for horizontal features and 32.5 nm for vertical features. Since in a real lithography process OPC would be used to correct for these systematic errors, mask bias was applied as needed per pitch for all subsequent simulations. The final H-V bias, after the proper application of OPC, is shown in Figure 5.

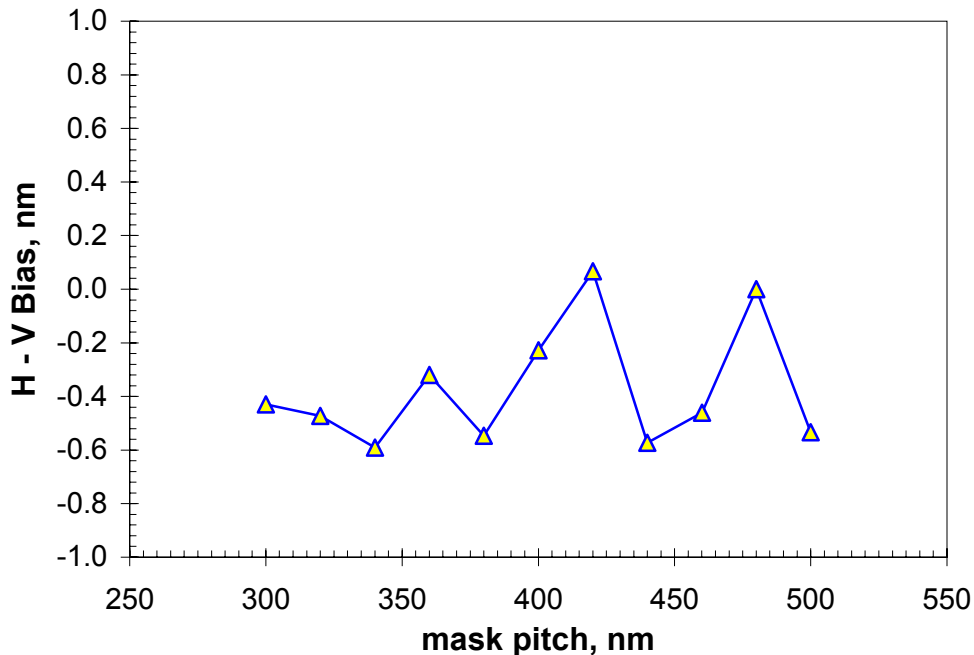


Figure 5. Residual H-V bias for 100 nm features after OPC was applied. No source errors are applied ($\lambda = 193$ nm, 0.92 NA, nominal dipole center $\sigma = 0.7$, radial $\sigma = 0.1$).

5. Dipole Source Telecentricity Error in x

With mask biasing applied to correct H and V features to 100 nm CD, a source telecentricity error was applied to the dipole in x by 0.05 sigma and resist CDs simulated across pitch and focus for the 100 nm H-V lines and 75 nm V lines.

Source telecentricity error in x causes the appearance of H-V bias in the 100 nm lines of up to -8 nm depending on pitch (Figures 6 and 7). Horizontal CDs decrease up to -8 nm with worst CD reduction occurring at 360 nm pitch. Vertical CDs increase by about 2 nm depending on pitch. Vertical 100 nm lines also exhibit an approximately linear placement error through focus (Figure 8). Simulations of 75 nm vertical lines show an even stronger dependence of placement error upon focus and x telecentricity error over -0.05 to 0.05 sigma offset (Figure 9). The placement error is about linear through focus and forms a saddle through x telecentricity error with maximum placement error of about ± 30 nm over the full process window.

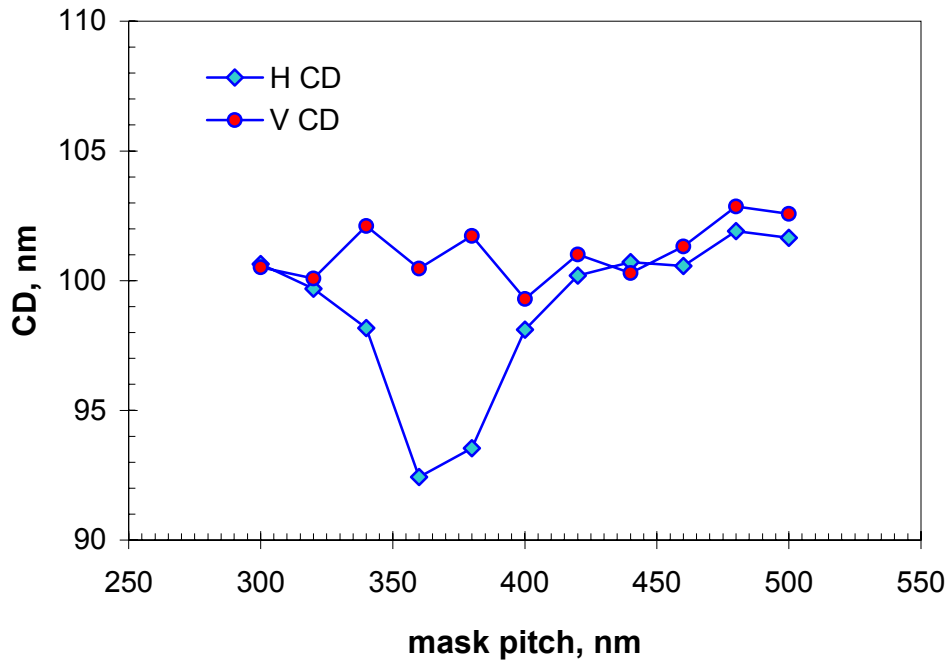


Figure 6. H & V CDs for 100 nm features (after mask bias) vs. pitch with 0.05 sigma x-telecetricity error applied ($\lambda = 193$ nm, 0.92 NA, nominal dipole center $\sigma = 0.7$, radial $\sigma = 0.1$).

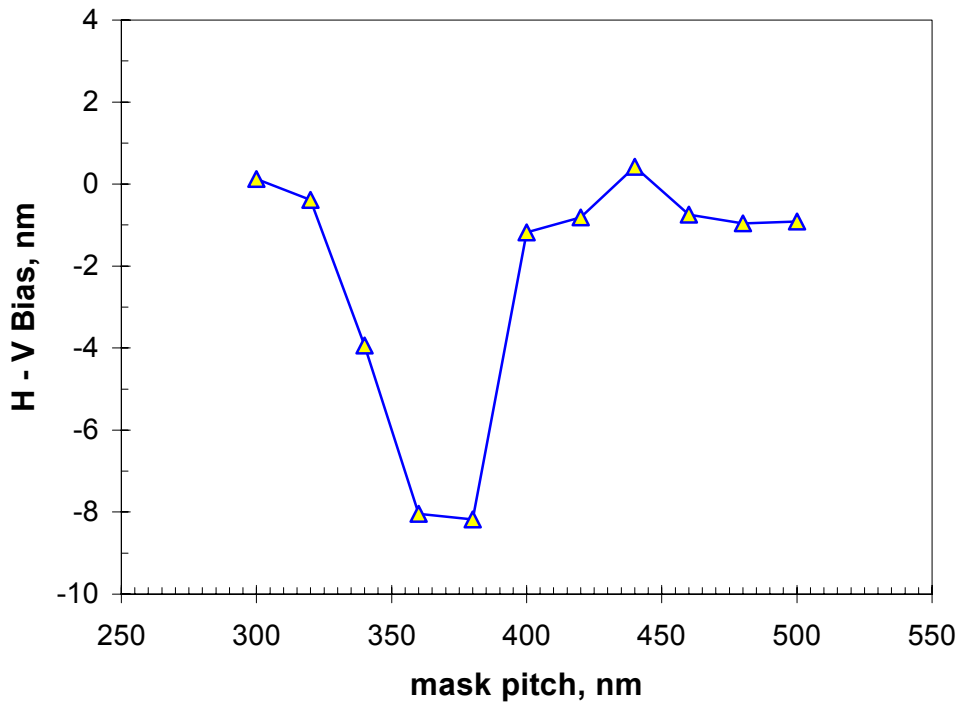


Figure 7. H-V Bias vs. pitch for CDs for 100 nm H-V CD with 0.05 sigma x-telecetricity error applied ($\lambda = 193$ nm, 0.92 NA, nominal dipole center $\sigma = 0.7$, radial $\sigma = 0.1$).

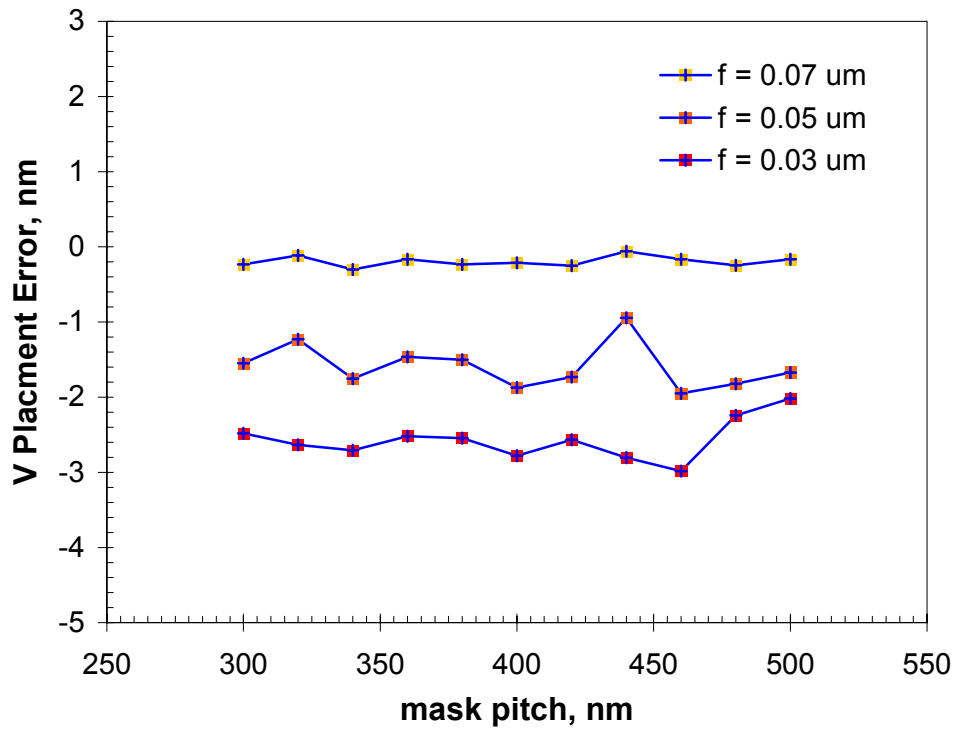


Figure 8. Vertical 100 nm line placement error vs. focus and pitch with 0.05 sigma x-telecentricity error applied ($\lambda = 193$ nm, 0.92 NA, nominal dipole center $\sigma = 0.7$, radial $\sigma = 0.1$).

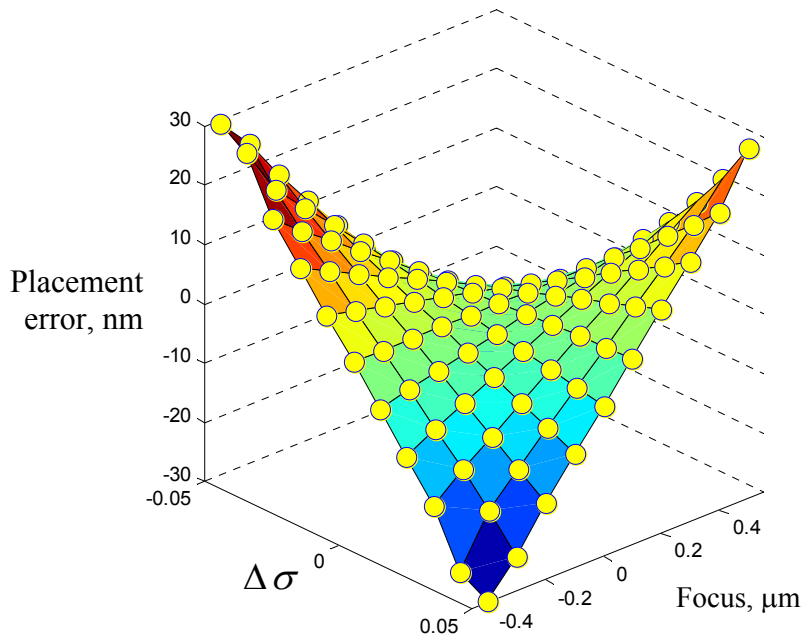


Figure 9. Vertical 75 nm line, 150 nm pitch placement error vs. focus with ± 0.05 sigma x-telecentricity error applied ($\lambda = 193$ nm, 0.92 NA, nominal dipole center $\sigma = 0.7$, radial $\sigma = 0.1$).

No placement errors are observed for the horizontal 100 nm lines. The strong sensitivity of placement error upon dipole x-telecentricity error observed for the vertical 75 nm lines might be considered as a way to diagnose source shape errors.

6. Application of Dipole Source Telecentricity Error in y

Source telecentricity error in y causes the appearance of H-V bias of again up to -8 nm, depending on pitch. Horizontal CDs are most affected and decrease up to -8 nm with worst CD reduction occurring again at 360 nm pitch. Vertical CDs generally do not change nor do they exhibit placement errors. Horizontal lines exhibit placement error about quadratic through focus with curvature and concavity or convexity increasing with defocus. Simulations of 75 nm vertical lines on 150 nm pitch show no placement error.

Generally, the observations are the converse of observations with x telecentricity error applied to the source. Figure 10 shows 100 nm horizontal and vertical CD vs. pitch with y -telecentricity source error applied; with H-V bias shown in Figure 11. Figure 12 shows the 100nm horizontal line placement error through focus and pitch.

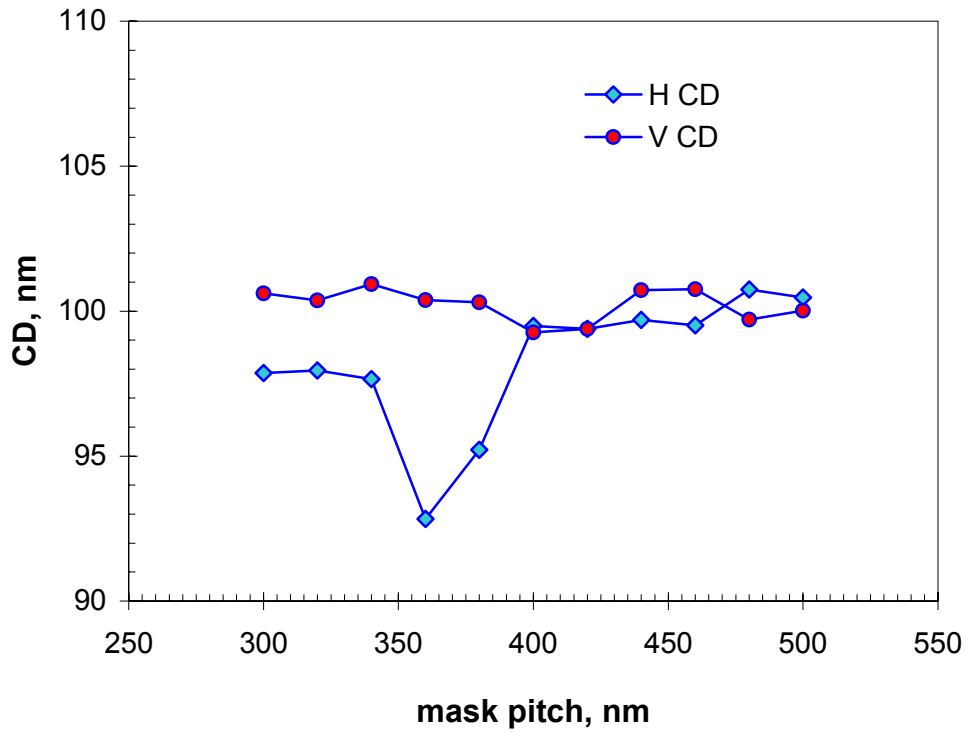


Figure 10. Horizontal and vertical 100 nm line CDs vs. pitch with 0.05 sigma y-telecentricity source error applied ($\lambda = 193$ nm, 0.92 NA, dipole center $\sigma = 0.7$, radial $\sigma = 0.1$).

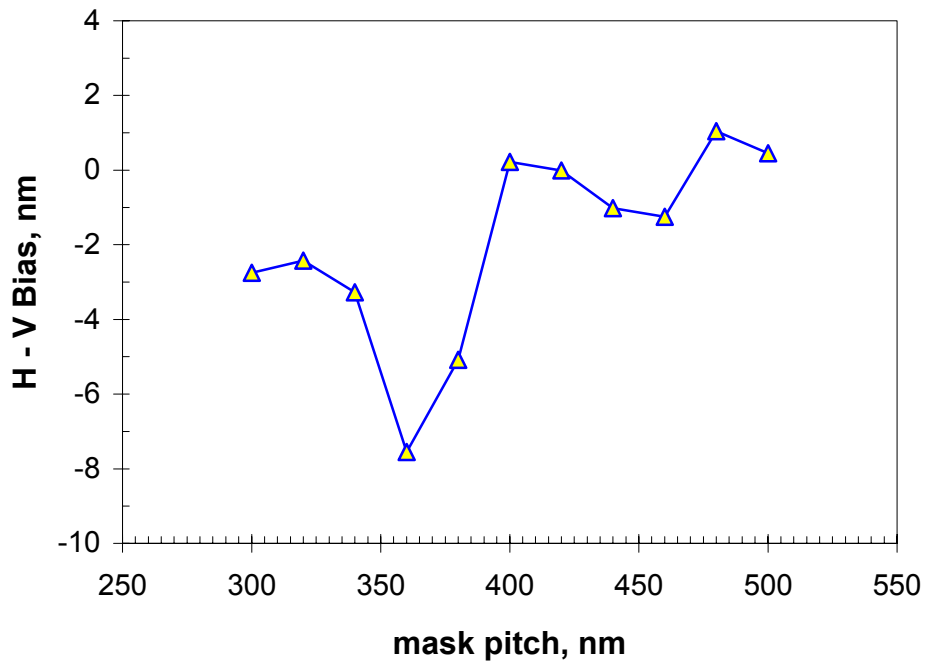


Figure 11. H-V Bias vs. pitch for CDs for 100 nm H-V CD with 0.05 sigma y-telecentricity source error applied ($\lambda = 193$ nm, 0.92 NA, nominal dipole center $\sigma = 0.7$, radial $\sigma = 0.1$).

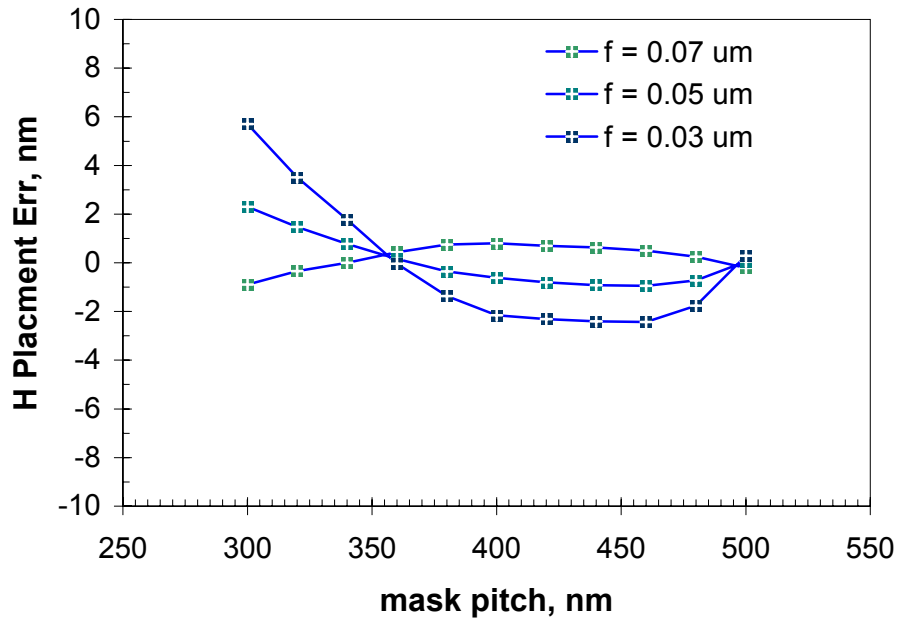


Figure 12. Horizontal 100 nm line placement error vs. focus and pitch with 0.05 sigma y-telecentricity source error applied ($\lambda = 193$ nm, 0.92 NA, nominal dipole center $\sigma = 0.7$, radial $\sigma = 0.1$).

7. Application of Unbalanced Pole Intensity Source Error

The 75 nm vertical lines and 100 nm horizontal and vertical lines were simulated with unbalanced pole intensity: left pole intensity is 0.5 while right pole intensity is 1. The error affects vertical line CDs which fluctuate about the nominal 100 nm by ± 2 nm depending on pitch (Figure 13). Vertical lines 300 nm – 500 nm pitch also exhibit placement errors about linearly through focus with worst case -6 nm (Figure 15), although vertical 75 nm lines on 150 nm pitch exhibit only small placement errors with worst case 0.5 nm when left pole intensity is zero. Horizontal lines show no placement errors and only small (< 1 nm) CD changes about 100 nm (Figure 16).

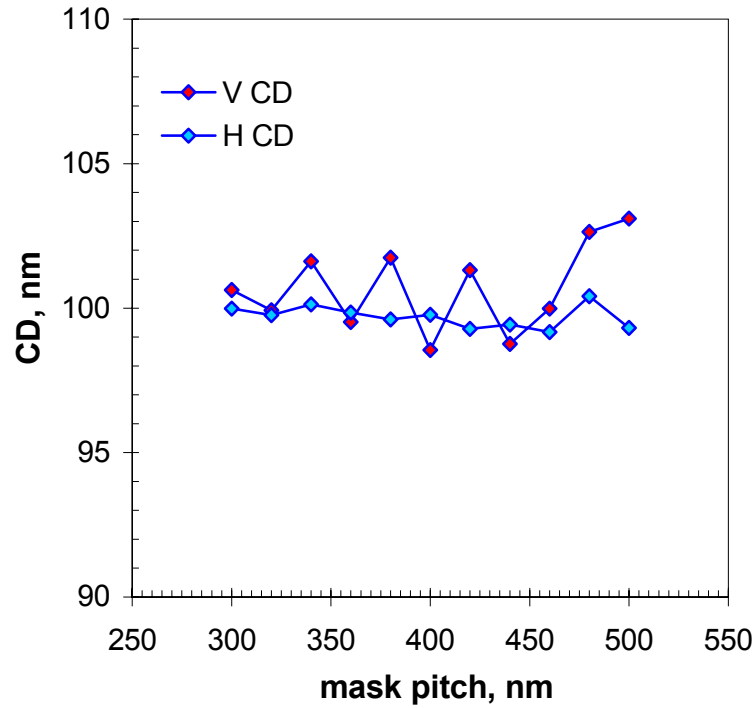


Figure 13. Horizontal and vertical CD vs. mask pitch for 100 nm features with unbalanced pole intensity source error applied ($\lambda = 193$ nm, 0.92 NA, nominal dipole center $\sigma = 0.7$, radial $\sigma = 0.1$).

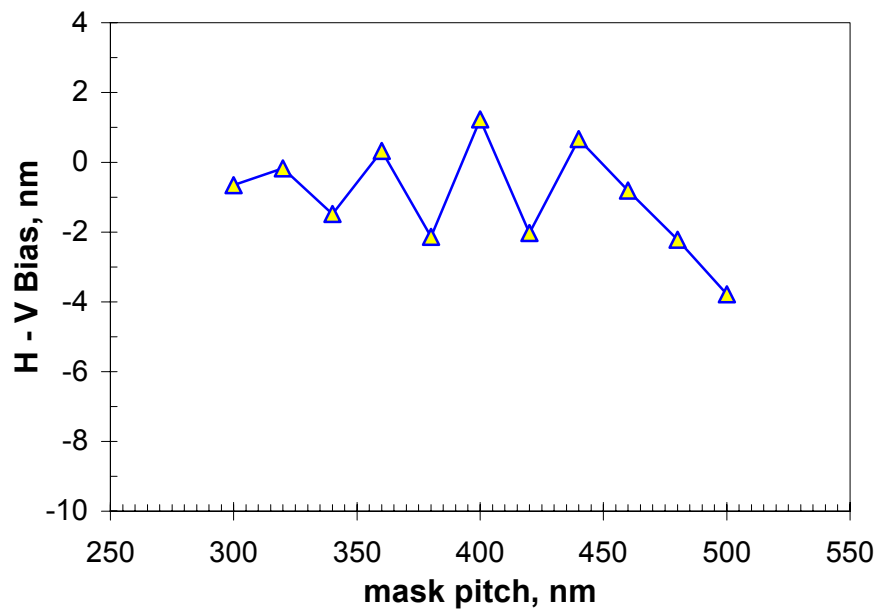


Figure 14. H-V Bias vs. mask pitch for 100 nm features with unbalanced pole intensity source error applied ($\lambda = 193$ nm, 0.92 NA, nominal dipole center $\sigma = 0.7$, radial $\sigma = 0.1$).

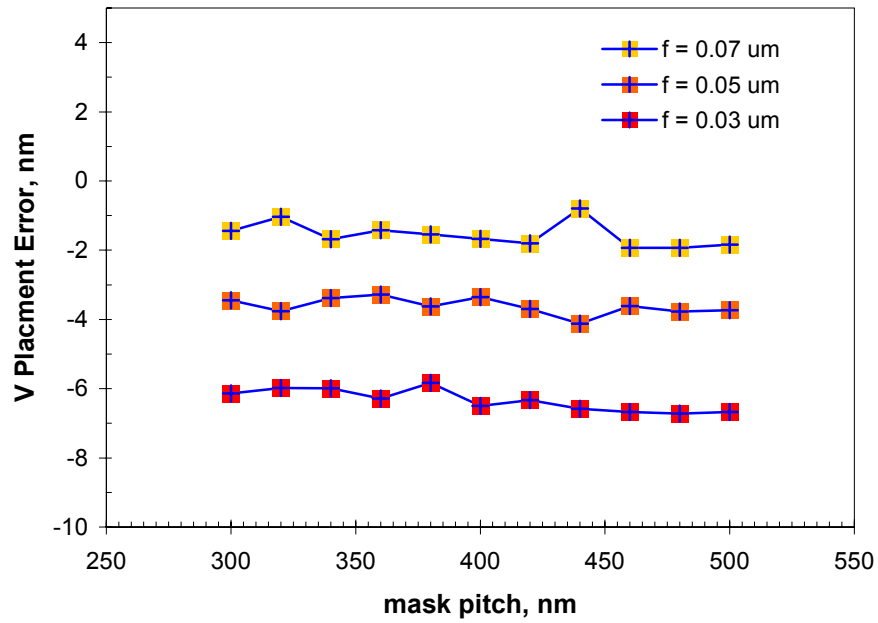


Figure 15. Vertical line placement error vs. focus and mask pitch with unbalanced pole intensity source error applied ($\lambda = 193 \text{ nm}$, 0.92 NA , nominal dipole center $\sigma = 0.7$, radial $\sigma = 0.1$).

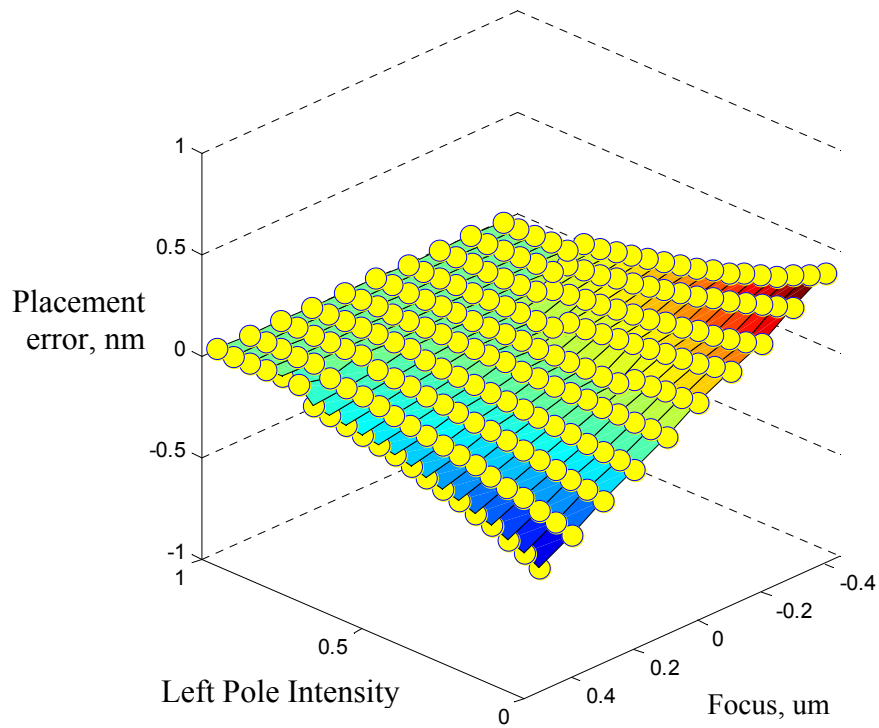


Figure 16. 75 nm V line, 150 nm pitch placement error vs. focus and left pole intensity ($\lambda = 193$ nm, 0.92 NA, nominal dipole center $\sigma = 0.7$, radial $\sigma = 0.1$).

8. Application of Rotational Source Error

Resist CDs for vertical 75 nm dense lines and 100 nm vertical and horizontal lines were simulated with 5 degrees of counter-clockwise rotational source error applied. Only horizontal 100 nm line CDs were affected with worst CD reduction at the 360 nm pitch (Figure 17). No horizontal or vertical line placement errors were observed.

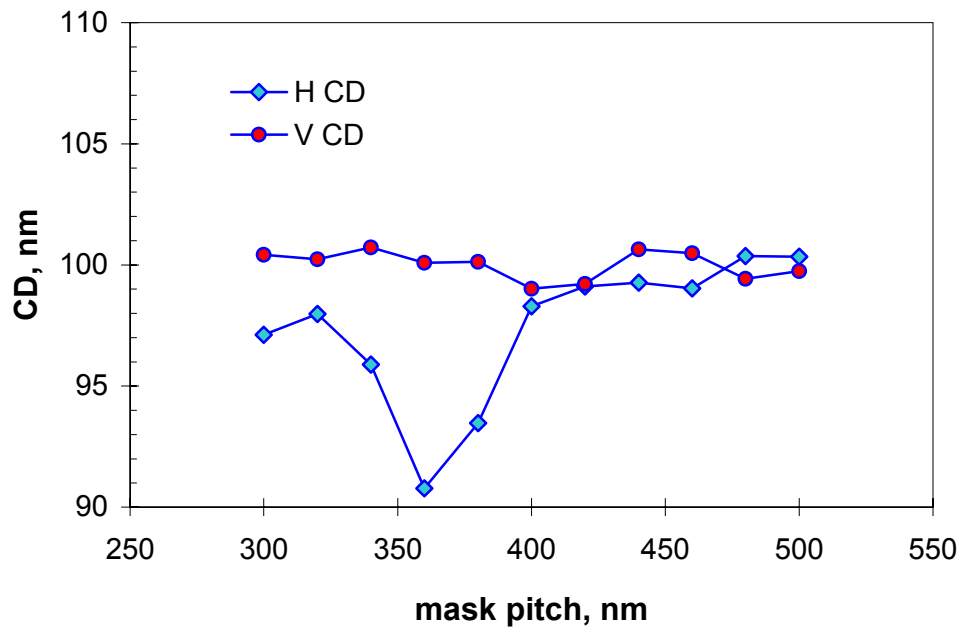


Figure 17. Horizontal and vertical 100nm line CD vs. pitch for a rotational source error ($\lambda = 193$ nm, 0.92 NA, nominal dipole center $\sigma = 0.7$, radial $\sigma = 0.1$).

9. Discussion

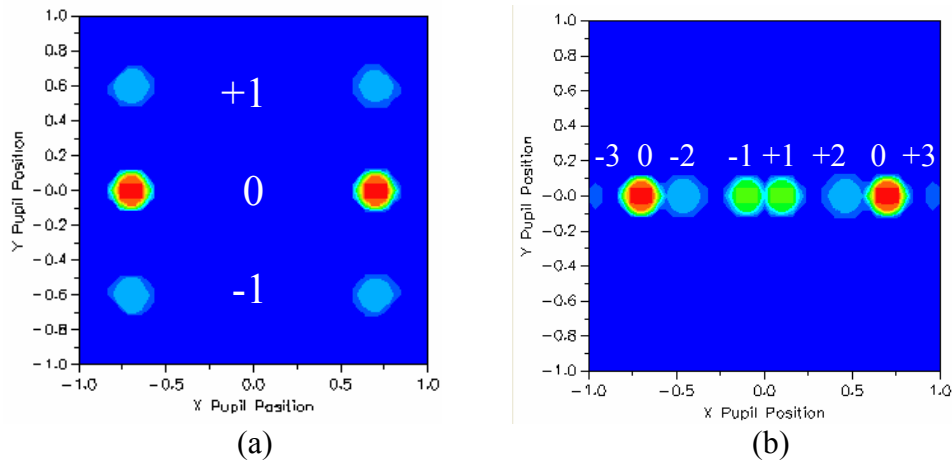
H-V bias is observed for all source errors examined with worst case of about -10 nm depending on pitch for the peripheral 100 nm features. Generally, horizontal lines show the most sensitivity and in particular, those H lines thereabout 360 nm pitch. Why should the 100 nm horizontal line at 360 nm pitch be most sensitive? How does H-V bias arise?

Simulations of the source diffraction pattern with no source error applied reveal that the edge of the \pm first diffraction order is placed at the pupil edge. As shown in previous work, the pitch that just allows only three beam imaging for a given source is the pitch that is most sensitive to a shift in the source position. Figure 18 shows the source diffraction pattern for 100

nm horizontal and vertical lines at 360 nm pitch with and without x -telecentricity source error applied. The first diffraction orders are observed to lie just inside the pupil. Shifting the position of the dipole forces the first diffraction order to be clipped by the pupil edge, and causes some fractional 2-beam imaging, depending on direction and magnitude of displacement. Horizontal or x -oriented source telecentricity errors reduce the integral of the partially-coherent diffraction order amplitude in the pupil equally on both sides of the horizontal line, resulting in CD reduction. A vertical, or y -oriented source telecentricity error changes this integrated amplitude preferentially on one side of the horizontal line, resulting in placement error through focus.

In the case of vertical lines, the diffraction pattern is spread along the x -axis and behavior is more complicated, since, depending on pitch, many orders may be present in the pupil. An x -oriented source telecentricity error causes the n^{th} diffraction order(s) to be clipped by the pupil, resulting in x -oriented asymmetry in the diffraction pattern.

H-V bias was shown in the first paper (in the context of partially-coherent source telecentricity error) to be dependent on the ratio of 2-beam to 3-beam imaging¹, depending on line orientation; this principle holds with respect to dipole source errors, except that the number of diffraction orders in the pupil may be higher than 3, especially in the case of vertical y -oriented lines at relaxed pitch, where the pupil may approach saturation. Generally, the case of more complex sources, H-V bias arises from the ratio of n -beam : $(n+1)$ -beam imaging for horizontal and vertical lines.



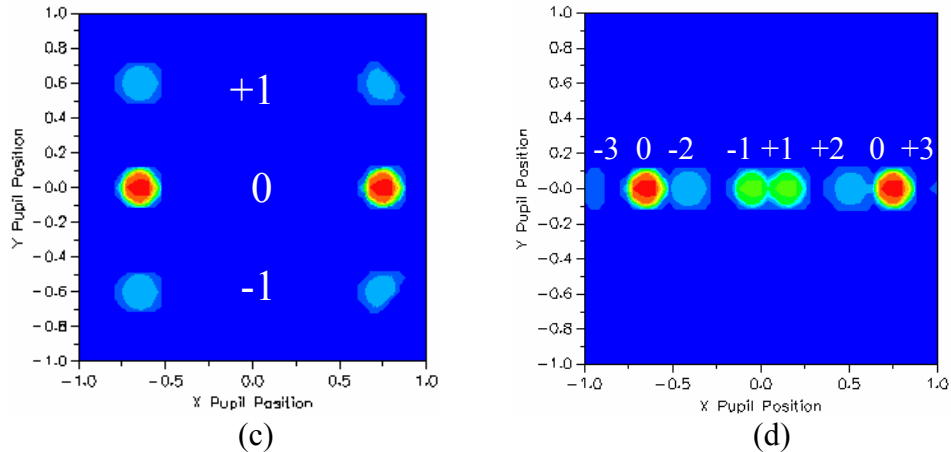


Figure 18. 100 nm horizontal and vertical line source diffraction pattern, 360 nm pitch, with and without 0.05 sigma source x-telecentricity error applied. a) horizontal lines, no source error; b) vertical lines, no source error; c) horizontal lines, 0.05 sigma source x-telecentricity error; d) vertical lines, 0.05 sigma source x-telecentricity error. Ratio of n -beam imaging changes with line orientation and source error, producing H-V bias effects.

10. Conclusions

After astigmatism coupled with defocus, illumination source shape errors are the most frequent cause of H-V bias¹. A dipole source with circular poles presents an inherent H-V bias according to simple diffraction theory and the geometry of the circle; for this x -oriented dipole, the minimum vertical pitch that may be imaged was very roughly half the minimum horizontal pitch that may be imaged. Mask OPC must be used to correct the inherent H-V bias at pitches which image at both horizontal and vertical orientations. However, after OPC, in all cases examined, dipole source shape errors produced H-V biasing through pitch (and probably focus) and placement errors through focus. Source errors, such as telecentricity error, can cause a change in the ratio of n -beam imaging for horizontal lines to $(n+a)$ -beam imaging for vertical lines, producing H-V bias. The most sensitive pitch for a given source error will be the pitch that puts all of the first order just inside the lens. The results should be similar for other source shapes and source errors.

11. References

1. C.A. Mack, "The Causes of Horizontal-Vertical Bias in Optical Lithography", Fuji Film Interface Interface Proceedings, 2005
2. D.S. Goodman and A.E. Rosenbluth, "Condenser Aberrations in Köhler Illumination", *Optical/Laser Microlithography, Proc.*, SPIE Vol. 922 (1988) pp. 108-134.
3. G.J. Stagaman, R.J. Eakin, J.C. Sardella, J.R. Johnson, C.R. Spinner, "Effects of Complex Illumination on Lithography Performance", SPIE Vol. 2726 (1996) pp. 146-157.
4. S.P. Renwick, S.D. Slonaker, I. Lalovic, K. Ahmed, "Influence of Laser Spatial Parameters and Illuminator Pupil-Fill Performance on the Lithographic Performance of a Scanner", *Optical Microlithography XV, Proc.*, SPIE Vol. 4691 (2002) pp. 1400-1411.

5. G. Zhang, C. Wang, C. Tan, J. Ilzhoefer, C. Atkinson, S.P. Renwick, S.D. Slonaker, D. Godfrey, C. Fruga, "Illumination Pupil Fill Measurement and Analysis and its Application in Scanner V-H Bias Characterization for 130nm Node and Beyond", *Optical Microlithography XVI, Proc.*, SPIE Vol. 5040 (2003) pp. 45-56.
6. C. Hwang, I.S. Kim, S.G. Woo, H.K. Cho, W.S. Han, "Impact of Illumination Intensity Profile on Lithography Simulation", *Optical Microlithography XVII, Proc.*, SPIE Vol. 5377 (2004) pp.1427-1434.
7. J. Shin, S. Lee, H. Kim, C. Hwang, S.S. Kim, S.G. Woo, H.K. Cho, J.T. Moon, "Measurement Technique of Non-telecentricity of Pupil-fill and its Application to 60nm NAND Flash Memory Patterns", *Optical Microlithography XVIII, Proc.*, SPIE Vol. 5754 (2005) pp.294-302.